RIGA TECHNICAL UNIVERSITY

Artis Riepnieks

PARAMETER ESTIMATION AND SIGNAL MODELLING FOR PHASOR MEASUREMENT UNITS

Summary of the Doctoral Thesis

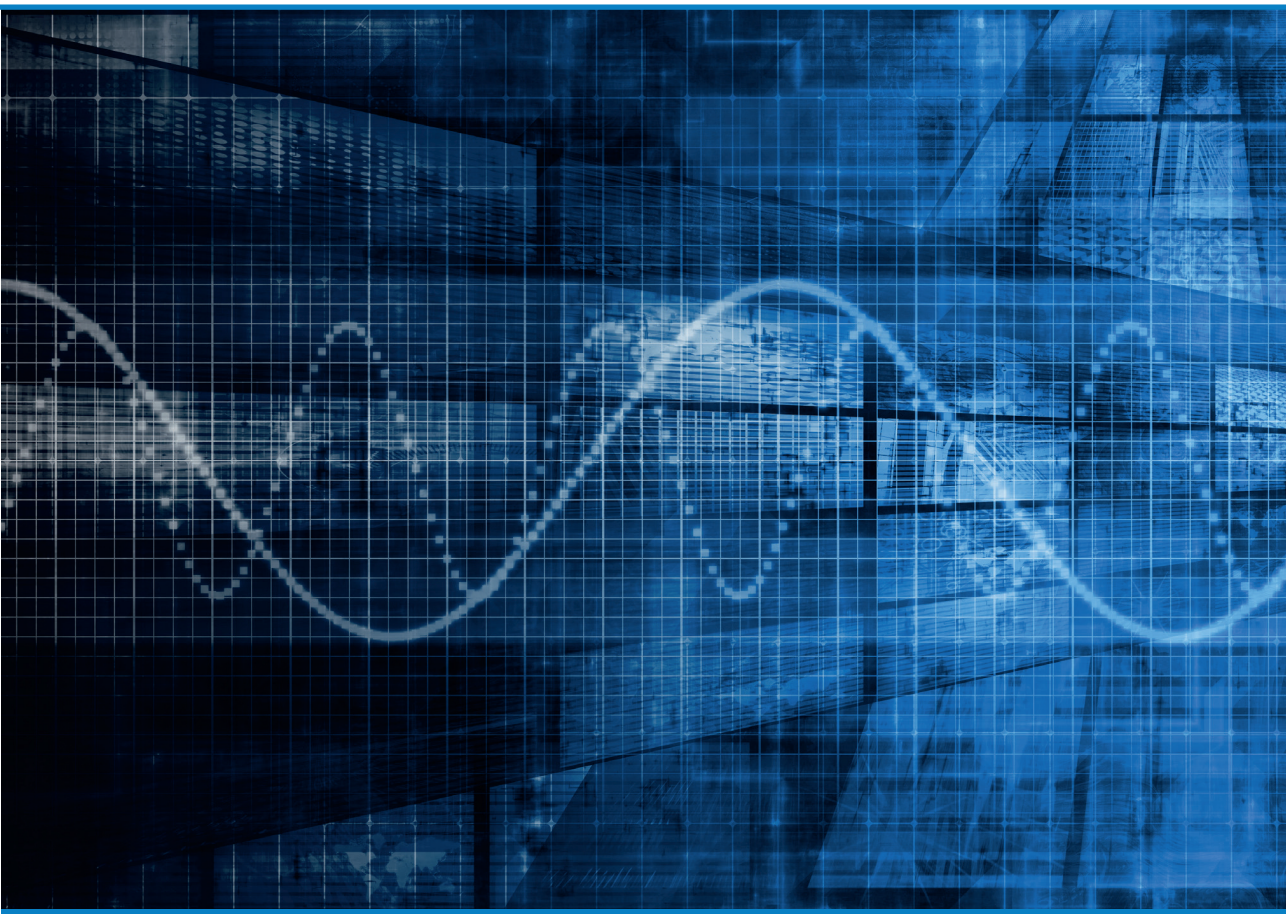

RTU Press
Riga 2018

RIGA TECHNICAL UNIVERSITY
Faculty of Power and Electrical Engineering
Institute of Computerized Control of Electrical Technology

Artis Riepnieks
Doctoral Student of the Study Programme "Computerized Control of Electrical Technology"

PARAMETER ESTIMATION AND SIGNAL MODELLING FOR PHASOR MEASUREMENT UNITS

Summary of the Doctoral Thesis

Scientific supervisor
Professor *Dr. habil. sc. ing.*
LEONĪDS RIBICKIS

Scientific advisor
Dr. sc. ing
HAROLD KIRKHAM

RTU Press
Riga 2018

Riepnieks, A. Parameter Estimation and Signal Modelling for Phasor Measurement Units. Summary of the Doctoral Thesis. Riga: RTU Press, 2018. 48 p.

Published in accordance with the decision of Promotion council of August 30, 2018, Minutes No. 2018-4 (66).

ISBN 978-9934-22-168-2 (print)
ISBN 978-9934-22-169-9 (pdf)

DOCTORAL THESIS PROPOSED TO RIGA TECHNICAL UNIVERSITY FOR THE PROMOTION TO THE SCIENTIFIC DEGREE OF DOCTOR OF ENGINEERING SCIENCES

To be granted the scientific degree of Doctor of Engineering Sciences, the present Doctoral Thesis has been submitted for the defence at the open meeting of RTU Promotion Council on December 7, 2018 at the Faculty of Power and Electrical Engineering of Riga Technical University, Azenes street 12 k-1, room 212.

OFFICIAL REVIEWERS

Professor *Dr. sc. ing*. Oskars Krievs
Riga Technical University

Research engineer *Dr*. James Follum
Pacific Northwest National Laboratory, USA

Dr. sc. ing Antons Kutjuns
Riga Technical University

DECLARATION OF ACADEMIC INTEGRITY

I hereby declare that the Doctoral Thesis submitted for the review to Riga Technical University for the promotion to the scientific degree of Doctor of Engineering Sciences is my own. I confirm that this Doctoral Thesis had not been submitted to any other university for the promotion to a scientific degree.

Artis Riepnieks ……. (signature)
Date: ……

The Doctoral Thesis has been written in English. It consists of Introduction; 5 chapters; Conclusion; 58 figures; 2 tables; 2 annexes; the total number of pages is 91. The Bibliography contains 60 titles.

CONTENTS

Overall description of the Doctoral Thesis

Relevance of the topic

Since the very beginnings of Alternating Current (AC) systems in late 1880s [1] it was apparent that the system must be in balance between generation and load, otherwise the voltage and frequency will swing widely, that can damage devices and make the entire system unstable. Some would argue that since then the current day power grid is the largest man-made machine [2], [3], however its complexity cannot be overlooked. Modern power grid consists of millions of moving and stationary parts, variety of signals (including control signals) and, of course, electric power, that is the cornerstone of any modern society. Overall demand for power is ever increasing and large scale outages and blackouts are considered cataclysmic events.

In order to keep system running and lights on, the system must be kept at balance, but it is an increasingly difficult task to accomplish. Distributed renewable energy generation, uneven load patterns – power line load congestions and overloaded transformers, are common these days. In order to keep up with increasing power demand, generation/load uncertainties and the requirement for continuous supply, a new breed of measurement device was designed in 1992 – a phasor measurement unit (PMU). Based on 1983 idea proposed by A. Phadke, J. Thorp and M. Adamiak [4] of phasor measurements the device was capable to report real time system frequency 30 times per second (for 60Hz system). Compared to SCADA average 4 second latency, this is almost real time and allows for real-time actions to be carried out to ensure system integrity. All major power system operators have been deploying PMUs since then [5], including Latvia where JSC "Augstsprieguma tīkls", have been investing in PMUs since 2009. Possibilities with PMUs do not stop there, and enormous effort has been put for introduction of PMUs for distribution network [6] (where usually distributed small-scale generation is located and islanding modes are more relevant).

Capabilities offered by PMU are very valued and required during outage investigations, outage prevention and system work mode management. Yet, under IEEE standard [7] PMUs are struggling with the measurement that had implications of being one of most useful – rate of change of frequency (ROCOF). Issues were so severe that the standard got amended [8] and device under test is allowed to skip reporting ROCOF during ROCOF change.

This work is dedicated to provide a proof of concept for a new approach of making improved phasor (and phasor-like) measurements based on hypothesis that the act of measurement is actually the same as solving an equation. This is an idea of Dr. Harold Kirkham. During research the SEMPR (Signal Estimation by Minimizing Parameter Residuals) is developed and real-world signals as well as synthetic data is analyzed for research in ROCOF measurement sensibility. The present Thesis touches

also philosophical questions of real world and conceptual models and basis of metrology.

As part of research a new metric, called Goodness of Fit, is defined in order to improve PMU reports and our understanding of real situation in the network. Also, first experimental results for sampling variance are provided, showing an optimum for sampling rates for different noise affected signals.

Practical implications of the work presented can affect digital measurements from digital multi-meters to PMUs and calibration equipment in laboratories.

Based on results provided the idea can be applied over majority of digital measurement field and a concept for double-exponent model is provided as an example for future research.

Goals of the work and main tasks

The goal of the Doctoral Thesis is to prove a new measurement hypothesis (the act of measurement is equivalent of solving an equation) and make a working concept model for phasor measurement units.

Main tasks:

- to develop a mathematical model for electric signal parameter estimation;
- to develop a solver for estimation-based measurements;
- to analyze noise stability of the model;
- to analyze the obtained real-world signals;
- to make statistical analysis of obtained results in order to determine stability of the model;
- to propose full or partial implementation of the method in real PMU devices.

Scope and object of the research

The scope of the work is the power grid and its main measurements in a form of a phasor (input for phasor measurement units). The main research object is a new proposed method for performing phasor-like measurements faster and with higher confidence.

Scientific novelty of the work

- Dr. Kirkham's idea of “intelligent measurements” introduced a significant discovery. In this work the idea is applied to phasor measurements.
- SEMPR method has been developed for easy and accessible signal parameter estimation.
- Goodness of Fit (GoF) metric is introduced to give measurements a degree of credibility.
- An experimental statistical analysis, called sampling variance, is introduced and analyzed with SEMPR.

Practical significance of the work

- This work and intelligent measurements have practical implications in all applications where digital sampling and signal processing is performed.
- The introduced metric GoF in dB is implementable in any signal processing measurement device to indicate a level of trust one can put in a measurement to explain observed physical phenomenon. It has already been implemented in a real PMU device for testing [9].
- Statistical analysis performed in the work can help better understand the noise contents in the power grid and analyze their impact on measurements to improve them. Statistical analysis, just like GoF can be performed in the same device.
- SEMPR can be easily implemented with any measurement device with sufficient processing power to measure wide range of different signals, since the measurement models are easily changed and adjusted. Together with GoF it is possible to fine-tune the model to get the best estimates for signal parameters, e.g. adding harmonics and DC offset for phasor-like measurements in real PMU devices.
- Practical implications of the thesis are extremely wide, starting with electronic multi-meter to a PMU, testing equipment in laboratories, calibration equipment and finally in academic education – the way we teach modern metrology.

Methods and tools used

- Curve fitting method with bisquare weighted residual minimization was used for developing the concept of SEMPR.

- Additive sample and individual parameter noise injection methods were used for white Gaussian, Brownian motion, harmonics and DC offset noise implementation.
- Allan variance and introduced sampling variance statistical methods were used to describe estimator stability and noise effects.
- The code for SEMPR and parts of signal generation process were developed in MathWorks MATLAB software.

Thesis for defense

- An act of measurement is equivalent to solving an equation in a mathematical model set by physics.
- SEMPR can be practically implemented and is comparable to a real PMU capability.
- GoF is useful metric for stating a confidence level for any given measurement made by any PMU device.

Scientific publications

1. A. Riepnieks, H. Kirkham, L. Ribickis. Considerations for phasor measurement unit introduction in distribution system. 56th International Scientific Conference on Power and Electrical Engineering of Riga Technical University (RTUCON), 14–14 Oct. 2015, Riga, Latvia.
2. H. Kirkham, A. Riepnieks, E. So, J. McBride. Error correction: A proposal for a standard. Conference on Precision Electromagnetic Measurements (CPEM 2016). 10–15 July 2016, Ottawa, Canada.
3. H. Kirkham, A. Riepnieks. Dealing with non-stationary signals: Definitions, considerations and practical implications. IEEE Power and Energy Society General Meeting (PESGM). 17–21 July 2016, Boston, Massachusetts, USA.
4. A. Riepnieks, H. Kirkham. Rate of change of frequency measurement. 57th International Scientific Conference on Power and Electrical Engineering of Riga Technical University (RTUCON), 13–14 Oct. 2016, Riga, Latvia.
5. H. Kirkham, A. Riepnieks. Students' simple method for determining the parameters of an AC signal. 57th International Scientific Conference on Power and Electrical Engineering of Riga Technical University (RTUCON). 13–14 Oct. 2016, Riga, Latvia.
6. A. Riepnieks, H. Kirkham. An Introduction to Goodness of Fit for PMU Parameter Estimation. IEEE Transactions on Power Delivery. Vol. 32, 5, Oct. 2017, pp. 2238–2245.

7. A. Riepnieks, H. Kirkham, A. J. Farris, M. Engels. Phase jumps in PMU signal generators. IEEE Power & Energy Society General Meeting. 16–20 July 2017, Chicago, Illinois, USA.
8. H. Kirkham, A. Riepnieks, M. Albu, D. Laverty. The nature of measurement, and the true value of a measured quantity. IEEE International Instrumentation and Measurement Technology Conference (I2MTC). 14–17 May 2018, Houston, Texas, USA.

All papers are available online in scientific databases, including SCOPUS.

Other works

H. Kirkham, A. Riepnieks. Measurement of phasor-like signals. Pacific Northwest National Laboratory report prepared for the U.S. Department of Energy. June 2016, Richland, Washington, USA.

Conferences

1. 56th International Scientific Conference on Power and Electrical Engineering of Riga Technical University (RTUCON), 14–14 Oct. 2015, Riga, Latvia.
2. Conference on Precision Electromagnetic Measurements (CPEM 2016), 10–15 July 2016, Ottawa, Canada.
3. IEEE Power and Energy Society General Meeting (PESGM), 17–21 July 2016, Boston, Massachusetts, USA.
4. 57th International Scientific Conference on Power and Electrical Engineering of Riga Technical University (RTUCON), 13–14 Oct. 2016, Riga, Latvia.
5. IEEE Power & Energy Society General Meeting, 16–20 July 2017, Chicago, Illinois, USA.
6. IEEE International Instrumentation and Measurement Technology Conference (I2MTC), 14–17 May 2018, Houston, Texas, USA.

Research collaboration

Large part of the work was done in Pacific Northwest National Laboratory, Richland, Washington, USA, in collaboration with Dr. Harold Kirkham. The research in the USA was funded under Baltic American Freedom Foundation scholarship.

Scope and structure of the work

The work is dedicated to science of metrology and, more specifically, digitally sampled electrical measurements. Main emphasis is put on phasor measurement units and measurements of power system signal parameters and possible improvements.

The first chapter deals with philosophical questions and basis for the non-stationary power system waveform measurements. Nature must be separated from the conceptual models in one's mind, while keeping the model tractable and related to nature. Models can be re-adjusted, but nature – cannot.

The second chapter focuses on phasor measurement units, mathematical model underneath, and their use in power system synchronized measurements. Model limitations have been indicated and possible solutions offered.

The third chapter shows the mathematical and developed practical proof-of-concept for Kirkham equation-based model for phasor-like measurements in power system (Signal Estimation by Minimizing Parameter Residuals).

In the fourth chapter the limitations for SEMPR are explored with various synthetic signals, containing variations of noises and harmonics. Statistical analysis methods are implemented, and sampling variance is introduced. The chapter provides first experimental results on sampling variance for possible uses in real-world applications.

The fifth chapter contains results from real-world signals and PMU measurements, including a fault in extra-high voltage network. It is shown that SEMPR in general performs better with measurements over the fault sampled data than PMU. Results of statistical analysis are provided for real-world medium voltage distribution network signal.

The Doctoral Thesis has been written in English. It consists of Introduction; 5 chapters; Conclusion; 58 figures; 2 tables; 3 annexes; the total number of pages is 91. The Bibliography contains 60 titles

Outline of the work contents

Chapter 1. Analysis of Different Mathematical Models for Real- world Representation

1.1 Carnap equation and model

The most relevant notion to begin with is the Carnap quantitative language of a measurement, or in other words – labeling for different models. Consider two bodies

with length, for example pieces of wood a and b. If they are combined so that they are end to end lying in a straight line, the new physical entity is now a combination of two objects and have length that is the sum of the lengths of a and b. This sounds like additive rule for length. Unfortunately, quite often this rule is not satisfactory.

Carnap really stresses out the difference between the two worlds – physical and mathematical. The symbol for physical joining operation "∘" is then introduced. Correct way of expressing the joining of two lines then is

$$L(a \circ b) = L(a) + L(b). \tag{1.1}$$

The "=" is the bridge between the real, physical world and the conceptual or mathematical one.

Every periodic function has a frequency parameter, but frequency by definition "number of occurrences per unit of time" is something existing in real world as swinging pendulum or celestial cycles. Once we cross the "=" in Carnap equation (1.1) it becomes a variable in an equation of a wave function. There is a large difference and we should avoid confusing them at all times. For the purpose of this work the term "frequency" denotes second variable in wave function (symbol ω) and the physical property of this number should be put aside, since there are questions like:

- What is the frequency when frequency is changing?
- What is the frequency for a quarter of a cycle signal?

In this sense in this work "frequency" (if not said otherwise) is only true for the measurement window and is a parameter in an equation for a mathematical model.

1.2 Rutman models

Keeping in mind the distinction between the nature and our conceptual world J. Rutman put it this way:

> *"... models are used to represent the physical world which is so complex that many details are ignored in the model: otherwise, the latter would become intractable. On the other hand, properties that have no direct meaningful counterparts in the real world have to be included in the model to make it tractable (stationarity of random processes is a well-known example)."* [10]

So, we can add or remove parameters and assumptions to our conceptual models of reality, but have to always keep in mind that it does not change the reality

itself, just our understanding. If something changes in nature, we have to accommodate in our models, otherwise our knowledge of the phenomenon being observed will be completely wrong, yet measurement can still be very accurate.

The mathematical model of an oscillator is given with

$$V(t) = [V_0 + \xi(t)] \sin[2\pi\upsilon_0 t + \varphi(t)], \tag{1.2}$$

where V_0 is nominal amplitude, υ_0 is nominal frequency, $\xi(t)$ is random amplitude noise and $\varphi(t)$ is random phase noise.

What is the frequency when the frequency is changing? Can it be answered with instantaneous frequency?

Instantaneous angular frequency for (1.2) is

$$\omega(t) = \frac{\mathrm{d}}{\mathrm{d}t}\left(\omega_0 t + \varphi(t)\right) = \omega_0 + \frac{\mathrm{d}\varphi(t)}{\mathrm{d}t}, \tag{1.3}$$

where $\dot{\varphi}(t) = \frac{\mathrm{d}\varphi(t)}{\mathrm{d}t}$ is a random frequency fluctuation around the ideal value ω_0 [11].

There is stationarity problem for $\varphi(t)$ where theoretically the existence of $\dot{\varphi}(t)$ is at question. As Rutman concludes, one must be very careful when dealing with phase and frequency noises, since it may lead to a use of non-existent quantities. In this work SEMPR is made to operate with frequency, phase, and amplitude noises, but it is done controllably, keeping in mind the physical implications.

Instantaneous frequency can never be instantaneous since it always involves a finite averaging interval τ. The notion of frequency for a dot on a wave function is simply not possible and the same distinction must be drawn between mathematical frequency and physical frequency of a periodical wave.

1.3 Kirkham model

It is Dr. Kirkham's idea to show that the “message” coming from a measuring device has “meaning” and it must not be ignored unlike in Claude Shannon’s [12]. The equal sign in Equation (1.1) is the link between conceptual and real worlds, but it does not mean “is the same as”, instead it should be interpreted as “is the same value as'. Therefore, the physical frequency of repeating oscillations is not the same as the value for the frequency in a mathematical model, it is just a representation.

The same stands true not only for measurement, but also for signal generation. Dr. Kirkham shows that those are practically the same just in different directions in Carnap equation,

$$\overleftarrow{\text{signal generation}} \quad X(a \circ b) = X(a) + X(b) \quad \overrightarrow{\text{measurement}} \tag{1.4}$$

where measurement is an act of solving an equation for mathematical model values, but the process of signal generation moves information from the mathematical model into physical world. As Kirkham indicates, calibration, of course, involves both. The calibration block diagram is given in Figure 1.1 and [13].

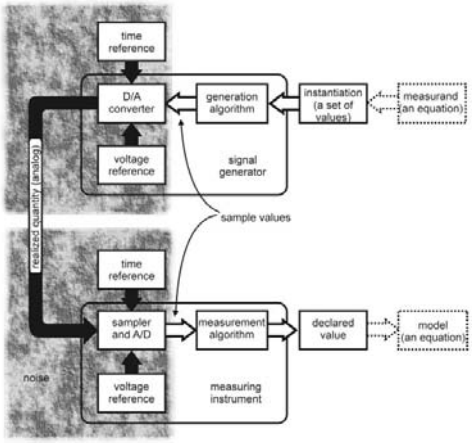

Fig. 1.1. Calibration block diagram.

On the left side there are real-world non-perfect and noisy signals, and on the right side is the conceptual mathematical world, that in both cases (measurement and generation) contains some mathematical models, made by our understanding of physics and mathematics.

Chapter 2. Synchronized Phasor Measurements in Transmission Network

Synchronized phasor measurements are becoming one of the most vital measurements of a modern power system.

With SCADA the measurements are captured every 4 seconds or so and from different areas they are not captured at the exact same time. System monitoring is essential during large disturbances and transient processes. In order to capture system dynamics and for fast real-time control/supervision faster capture periods and synchronized data is essential.

Synchronized phasor measurements mean that all measurements are using the same time reference and are synchronized with UTC (Coordinated Universal Time) using GPS (Global Positioning System) clocks [14]. With fast measuring rate (25 measurements per second in 50 Hz system) it is possible to monitor system transient processes. It is possible to discover blackouts, line tripping, generation unit dropping from network, FIDVR (Fault Induced Delayed Voltage Recovery) and other transient processes in real time as well as control the power system elements in real time to keep the system in balance.

Sine-wave between two adjacent buses will change the phase angle depending on the load, so by measuring synchronized phasors at both instances the P flow can be then computed (Fig. 2.1).

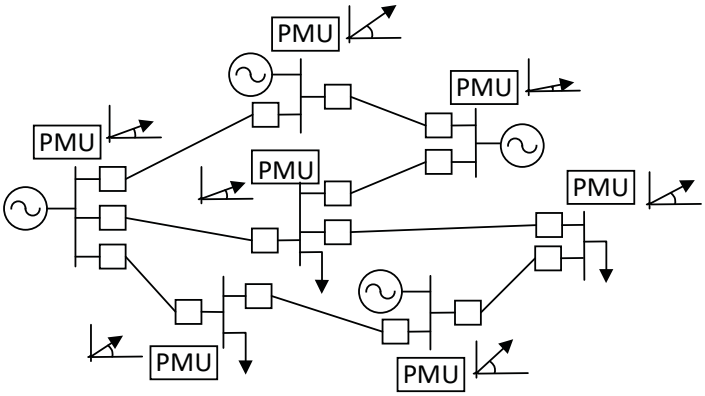

Fig. 2.1. Phasor angle measurements across power system.

Phasors are used for much more than just line load estimation. One implementation lies in control and protection domain, where phasors can be very useful [15], [16]. Stability depends on three factors: rotor-angle stability, frequency stability and voltage stability. Increasing complexity and interconnectivity of a modern power system [17] as well as larger penetration of distributed renewable energy sources [18] can create instability of the power system frequency. System oscillations at some circumstances can cause severe system instability, falling out of synchronism and blackouts [19].

2.1 Model of a phasor

A. Phadke, J. Thorp, and M. Adamiak proposed a new idea in their 1983 paper on how to measure frequency really fast and without counting signal zero-crossings [4].

Consider the exponential notation representing the sinusoid:

$$X_{\mathrm{m}}\mathrm{Re}\left[\mathrm{e}^{j(wt+\varphi)}\right] = X_{\mathrm{m}}\mathrm{Re}\left[X_{\mathrm{m}}\mathrm{e}^{j(wt)} + \mathrm{e}^{j(\varphi)}\right]. \quad (2.1)$$

where X_{m} is amplitude, ω is frequency, and φ is phase. In power applications, it is customary to omit the Re notation and to omit the frequency term, so that a sinusoidal input signal is written

$$x(t) = X_{\mathrm{m}}\mathrm{e}^{j\varphi}. \quad (2.2)$$

Note that the simplified equation of the sinusoid does not include the frequency. It includes only the stationary phasor.

Measuring phase angle and frequency is a hard thing to do (for real time applications). As shown by A. Phadke *et al.* in [4], it is possible to measure the difference in the phase angles between the recursive phase measurements and, by doing that, find the change in the frequency:

$$\frac{\mathrm{d}\psi}{\mathrm{d}t} = \frac{\psi_r - \psi_{r-1}}{(1/50N)}. \quad (2.3)$$

where ψ is derived from a "phase factor" $\mathrm{e}^{j\psi_r}$, the differentiated phase angle, r is recursive measurement, and N is sampling rate in samples per cycle.

A value called "rate of change of frequency" (ROCOF) was expected to be a very useful tool to indicate changes in the power system. In case of generation unit loss or line tripping, the frequency would be affected and ROCOF would indicate how fast the changes are. From change in the frequency between two recursive measurements ROCOF can be derived,

$$\frac{\mathrm{d}f}{\mathrm{d}t} = \frac{1}{2\pi}\frac{\mathrm{d}^2\psi}{\mathrm{d}t^2}. \quad (2.4)$$

where f is the frequency.

Note that the model of a phasor describes a sine-wave with static frequency and amplitude that is true from reference time to infinity of time. This is the mathematical model used in phasor measurement units (PMUs).

2.2 Synchro-phasor measurement units

PMU is a time synchronized measuring device reporting estimates of positive sequence voltage amplitude and phase angle, local frequency, and rate of change of frequency. A PMU prototype was developed in 1988 at Virginia Tech, USA, [20] and

in 1992, first commercial PMU was produced at Macrodyne Inc., USA, (Model 1690). In 1995, the first standard was developed, and most recent update was released in 2014 [8].

The input for any PMU is a filtered sine wave signal, that gets sampled and processed for synchronized measurements (Fig. 2.2).

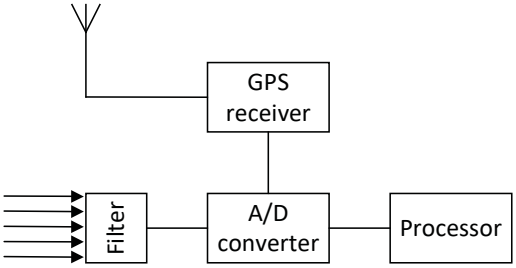

Fig 2.2. Main functional blocks of a PMU.

Actual measurement unit algorithms are commercial secrets for each PMU manufacturer, but in general at least some parts of digital signal processing are taking place in each and every one of them and are as follows:

- input signal is filtered;
- sampling rates can vary greatly (from 24 samples to 512 samples per cycle [21]);
- DFT is calculated;
- sampling may be synchronized with the UTC clock or the signal itself;
- phase angle differentiation is performed to calculate system parameters;
- parameters are time-stamped and forwarded to a data concentrator.

Discrete Furrier Transform (DFT) is calculated as in [14]:

$$x = \frac{\sqrt{2}}{N}\sum_{k=1}^{N} x_k \, \varepsilon^{\frac{-j2k\pi}{N}}, \tag{2.5}$$

where N is total number of samples in one period of the signal, x is the phasor, and x_k is the point-on-wave sample. Frequency-domain based calculations produce the positive sequence phasor

$$x_1 = |x_1|\varepsilon^{j\varphi}, \tag{2.6}$$

with an angular velocity exactly corresponding to the difference between system reference frequency and observed frequency. The system frequency is then

$$\omega = \omega_0 + \frac{d\varphi_1}{dt}. \tag{2.7}$$

While details of the phasor calculation techniques in PMUs are unknown to the public, for sure they include common key points: the output is 3 phase positive sequence voltage magnitude and angle, three phase positive sequence current magnitude and angle, local frequency (as deviation from nominal), rate of change of frequency, additional defined analog or digital signals (like transducer values, relay statuses or other flags). The accuracy of a PMU measurement is expressed in parts per unit as TVE (Total Vector Error) of a "perfect theoretical phasor" [22]. TVE is described in the standard [7]:

$$TVE(n) = \sqrt{\frac{\left(\hat{X}_r(n) - X_r(n)\right)^2 + \left(\hat{X}_i(n) - X_i(n)\right)^2}{\left(X_r(n)\right)^2 + \left(X_i(n)\right)^2}}, \tag{2.8}$$

where $\hat{X}_r(n)$ and $\hat{X}_i(n)$ are the sequences given by phasor estimates, $X_r(n)$ and $X_i(n)$ are theoretical values of the input signal at given time (n).

According to [8], the allowed TVE for a steady state test is 1 %, which means that there can be 1% difference between the observed phasor and theoretical phasor.

2.3 PMU limitations

Timing is very important in synchronized measurements. Allowed 1 % TVE error corresponds to ±31 µs time error in 50Hz system [8], therefore GPS clocks (or equivalent) are essential. PMU has to account for connection latency and delay of UTC signal to make synchronized A/D conversion. This becomes very important when comparing two different vendor PMUs because synchronization processes can be implemented differently (some A/D converters are phase locked to the system frequency).

Signal filtering is necessary in order to solve aliasing problems and also to remove any harmonic disturbances with any out of band signals. Filtering brings a delay that has to be taken into account. Using filtering across many windows the reported value is not entirely independent of previous, so there is a delay for reporting times because of the signal filtering [23], [24].

Interesting PMU performance indication can be found in G. Stenbakken and M. Zhou's paper (of 2007) and also in PMU standard amendment [8], [25]. The

standard under dynamic compliance (performance during ramp of system frequency) states:

> *"Measurements made during an exclusion interval shall not be used when determining measurement compliance. The exclusion interval is the time interval after the ramp leaves or before the ramp reaches the frequency range limit or a point where ROCOF changes."*

It is well known that the system frequency (therefore ROCOF) is changing all the time and at no point, it is static. Nevertheless, during testing the PMU can ignore windows when ROCOF is changing. In [25] (Fig. 2.3) it is experimentally showed how it looks in practice.

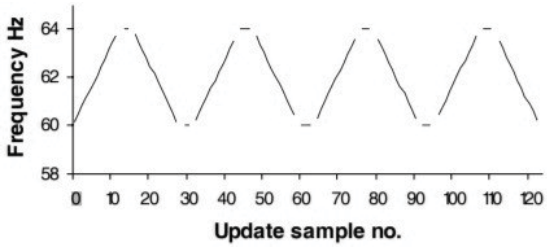

Fig. 2.3. Linear frequency ramp test signal *[25]*.

Transitions are closer investigated in [26]. It is shown that with Kirkham equation the transition process can be monitored.

In further research it was found that a curious phenomenon exist when input signal for such test is generated mathematically, e.g. using spreadsheet. Let us consider creating ramping frequency signal beginning with stationary signal (rate of change of frequency is zero) at t_0, and then at some given time point t_k introduce a rate of change of frequency. At t_k the rate of change of frequency starts to change the phase. The rate at which the frequency is changing is changing again (like in Fig. 2.3) at $t = t_m$. The spreadsheet continues to produce cosine describing sample numbers, but at t_m the phase has changed from $t = t_0$ so an unintentional phase jump is created.

This problem was named "van der Pol problem" during the research. The solution is simple and for each sample calculation the calculation must be done for new frequency and phase values in each step according to the following equation:

$$y(t) = A\cos\left(\int_0^t \omega \mathrm{d}t + \varphi\right), \tag{2.9}$$

where A is amplitude, ω is angular frequency, and φ is phase constant, but most importantly the argument of cosine function $(\omega t + \varphi)$ is the phase.

Chapter 3. Theoretical Background for Phasor-like Measurements

The classical phasor equation (2.2) describes a static sinusoidal signal that is true from the beginning of time till infinity, but this static situation is never true for real world signals.

Instantaneous frequency by definition cannot be measured [27]. This means we have to define a measurement window with more than one sample. This brings back the question about changing frequency.

A more suitable mathematical model than classical phasor is needed for representation of changing signals. B. Boashash [28] notes that a new meaning for the "frequency" parameter should be defined, because for nonstationary signals there is little sense talking about frequency.

3.1 Kirkham equation

In 2014, Harold Kirkham in his report at Pacific Northwest National Laboratory suggests to modify the equation of a phasor with additional parameters that would allow the signal to change:

$$x(t) = \left(X' + \frac{C'_X}{2}t\right)\cos\left\{\left(\omega' + \frac{C'_\varphi}{2} + \frac{C'_\omega}{2}t\right)t + \varphi'\right\}, \tag{3.1}$$

where each of phasor's parameters is modified with coefficients *C*. The linear change and the parameters of Kirkham equation apply only to a duration of measurement window (in contrast to phasor that holds true for $t = 0$ s to infinity).

3.2 Principles of a digital measurement

Digital measurement system is shown and described in [13]. In Fig. 3.1 basic structure of a digital measurement system is shown. Analog signal is sampled in A/D converter according to time reference and voltage reference. Point-on-wave data is processed by measurement algorithm, and declared value is presented. Note that, e.g. "apparent frequency" is true only for the measurement window and represents only the second parameter in the equation (model).

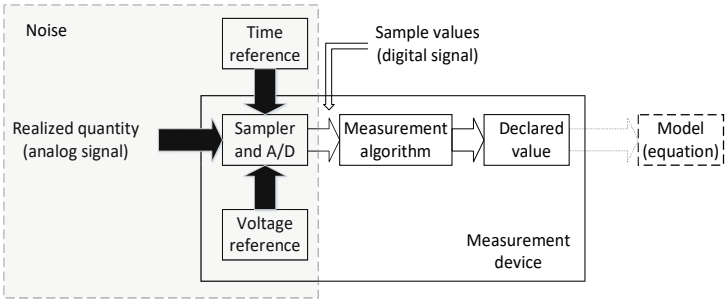

Fig. 3.1. Measurement system for digital measurement.

The “front end” (grey part in Fig. 3.1) is susceptible to noise, the “back-end” of the measurement system is more affected by “semantic coloration” [29] of an incomplete mathematical model for the measurement in the following cases.

- If the mathematical model for the measurement is erroneous and declared values do not represent the process observed.
- If the signal is affected by constantly present, but unforeseen disturbance. In this case there will be no representation for it in the model and measurement algorithms, therefore this value is not only ignored by measurement, but other declared values get affected by it.

This coloration could be a DC component of the AC signal measured in accordance to (3.1) in which case probably the declared value for amplitude would be altered slightly. Semantics is meaning, and semantic coloration is a **meaningful** mismatch between the observed reality and the model.

Using this notion, it would be possible and beneficial to implement an automatic self-calibration, e.g., after transducer change [30]. This would also improve measurement accuracy and device user experience.

3.3 Proof of concept

After the thought that the act of measurement is the same as equation solving the question becomes clear: what are the values that produce the real-world signal? Obvious method is curve fitting. By fitting the equation to the real observed signal the values are chosen that in the mathematical equation are the best fit and therefore can account for the signal observed. Software MATLAB of Mathworks Inc. was used to develop the fitting method for the proof of believable measurement concept.

Input data

The test signal is synthetically generated by using Microsoft Excel spreadsheet. For 50 Hz system, 30 samples per nominal cycle were used.

The mathematical model for the measurement is Equation (3.1) with added degrees of freedom for amplitude, frequency, and phase to change. The selected measurement window was 2 cycles.

To prove the model and measurement method, a signal with non-zero ROCOA (rate of change of amplitude) and ROCOF is used. ROCOA value is set to 0.1 pu/s and ROCOF is set to 3 Hz/s)

Variables for the signal generating equation are selected as follows:

- amplitude $X' =$ 1 pu;
- rate of change of amplitude $C'_x =$ 0.1 pu/s;
- frequency $\omega =$ 50 Hz;
- rate of change of frequency $C'_\omega =$ 3 Hz/s;
- phase $\varphi =$ 0 rad.

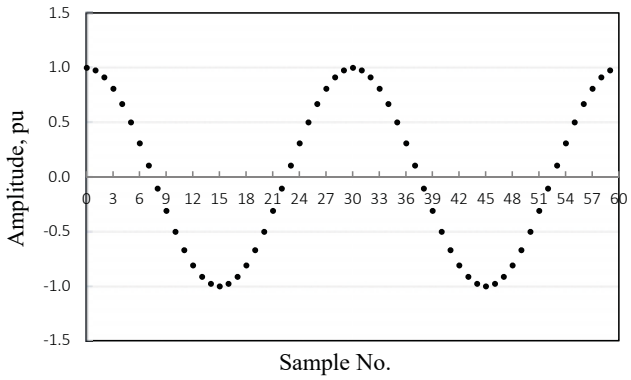

Fig. 3.2. Generated point-on-wave synthetic input data for the model with non-zero ROCOF and ROCOA.

Even though the changes are large (10 % change in amplitude and increase by 3 Hz of nominal frequency within a second), they are not noticeable with naked eye within one measurement window.

Measurement method

A nonlinear robust least squares fitting algorithm is selected, and MATLAB software is used to implement the measurement (solving) concept. It minimizes the summed square residuals that are the difference between the estimated data point Y_i and the observed signal value y_i. Based on the fact that the input signal is nonlinear, the method must approach the solution iteratively to lower the residual values.

The algorithm follows this procedure:

1. Start with a set of reasonable starting values. In normal operation, the values are the values at the end of a previous measurement window.
2. Calculate the Y_i values for the current set of input values.
3. Calculate a matrix of partial derivatives with respect to the values.
4. Weigh the residuals with the weighting algorithm.
5. Compute the weighted residuals.
6. Standardize the residuals
7. Calculate the weights. The final weight is the product of the two numbers produced by MATLAB, one called the "robust" weight and the "regression" weight.
8. Adjust the coefficients and determine whether the fit improves.
9. Iterate the process by returning to 2nd step until the fit reaches the specified convergence criteria [31].

Output

The result of the algorithm is a set of all values in the defined mathematical model. MATLAB also offers additional metrics for the algorithm, like iteration count, that can be used for evaluation of the performance of the particular algorithm.

The output for the input signal generated in Excel spreadsheet is spot-on. It is clear that the estimation with clean signals works with the precision of computer. Declared values for the input signal (Equation (3.1)) are as follows:

- amplitude $X' =$ 1 pu;
- rate of change of amplitude $C'_x =$ 0.1 pu/s;
- frequency $\omega =$ 50 Hz;
- rate of change of frequency $C'_\omega =$ 3 Hz/s;
- phase $\varphi =$ 0 rad.

Of particular interest is the parameter called Goodness of Fit (GoF), which is a number based on the residuals of the result of the measurement. Note that the use of GoF does not depend on the choice of measurement method. The number can be used as a metric and calculated by any PMU. In fact, the application does not stop there and GoF can be used in vast majority of other measurements with different measurement methods (as long as the observed quantity is available to compare to reconstructed mathematical model).

The residuals between the reconstructed (from obtained values) and generated waves show clearly (Fig 3.3) that the model and input signal are perfect match.

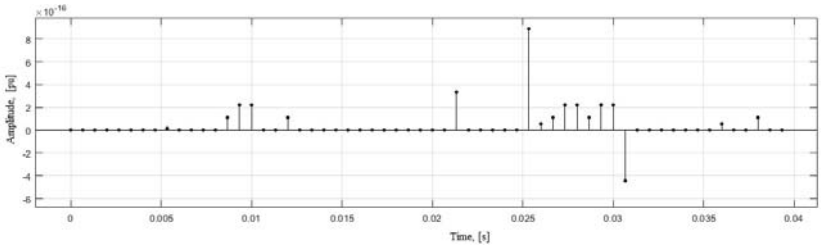

Fig. 3.3. Residuals from reconstructed point-on-wave data subtraction from the input data.

Residuals for the same input data but estimated with phasor model are at least 10^{13} times larger.

Goodness of Fit

The Goodness of Fit (GoF) proves to be a very useful tool coming out of the notion that the act of measurement is in fact solving the equation.

For ideal synthetically generated perfect signals (yet non-stationary) it is clear that perfect match can be achieved and residuals approach zero. The obvious answer for putting the method to the test is to try to estimate a signal that cannot be expressed in a single model (equation) for a whole measurement window, like a step-change in phase of a sinusoidal signal (Fig. 3.4).

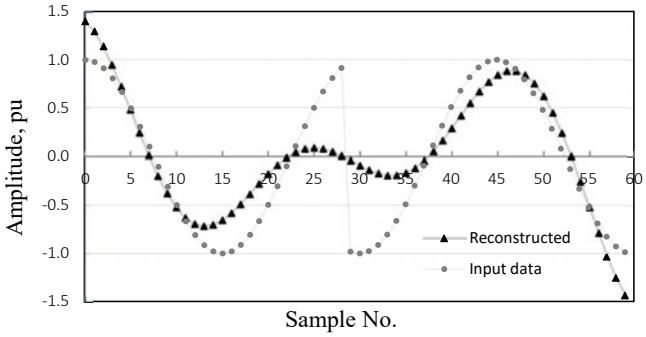

Fig. 3.4. Input signal with step change in phase and its estimated signal.

The method reports the values for the reconstructed signal. But is this something that anybody wants to know? If the actual input signal is given next to the measurement values, it is arguably useless – the match is clearly not good.

With GoF it would be possible to declare the confidence level for the measurement. In [32] GoF is introduced as reciprocal value of the fit standard error normalized and expressed in decibels:

$$GoF = 20\log\frac{X'}{\sqrt{\frac{1}{(N-m)}\sum_{k=1}^{N}(u_k - v_k)^2}}, \tag{3.2}$$

where N is the number of samples, m is the number of parameters being estimated in the equation, X' is the signal amplitude, u_k is the signal sample value and v_k is the estimated sample value. The parameter $(N - m)$ is called the residual degrees of freedom [33].

GoF calculated for the perfect signal in Fig. 3.2 is 304 dB, but in Fig. 3.4 it is 7 dB. The big difference is the reason for using logarithmic scale of decibels. This means that user confidence that the declared values really represent the reality should diminish. Further questions should be asked, like, what is going on in this particular measurement window? One information source is residuals.

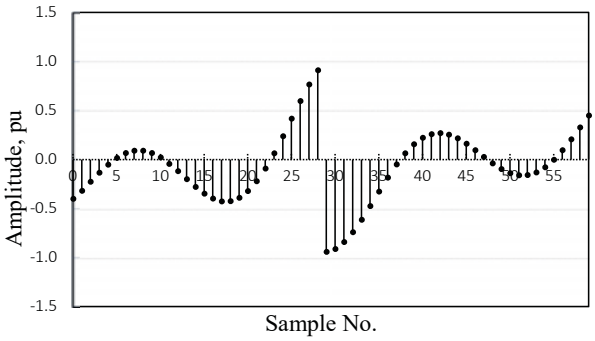

Fig. 3.5. Residuals from estimated signal and input signal with 180 degree phase jump.

The algorithm must make a choice, to align to the first part of sinusoid or the second part. In both occasions the declared values are not the ones for first half of signal or the second half, but the algorithm (PMU also) has to somehow find a reason for such signal behavior using the information that user has given to it (equation). In this case the best fit is if the signal is decreasing frequency very rapidly, to compensate for the jump in phase.

Estimation algorithm is called SEMPR or “Signal Estimation by Minimizing Parameter Residuals” (name given by Dr. Harold Kirkham).

Chapter 4. Analysis of the Phasor-like Model Limitations

In order to understand the limitations of the estimator algorithm, it would be beneficial to use no filtering at all. In theory noise influence should be less than

classical PMU because phase differentiation is not implemented, which is a very noise sensitive operation. The major benefit in this case also would be completely independent measurements (no overlapping measurement windows with no filtering).

Noise in the power grid is very well known as a fact yet very little understood process. There are many kinds of "noises", like harmonics, random noise, large disturbances, etc., and some of them contribute most of the time. This process is in addition to semantic coloration discussed earlier, but both of them contribute to the error.

4.1 Noise types and their effects

For signal generation purposes there are different kinds of noise models available (usually they are given the names or colors), but for PMU model it only makes sense to use the ones actually found in power system. Those are:

- harmonics;
- Gaussian white noise;
- Brownian noise (also known as *red noise* or *random walk*);
- DC offset.

Harmonics are defined as a sum of infinite number of oscillating functions:

$$f(x) = \frac{1}{2}a_0 + \sum_{n=1}^{\infty} a_n \cos(n\omega t) + \sum_{n=1}^{\infty} b_n \sin(n\omega t), \tag{4.1}$$

where $\frac{1}{2}a_0$ is the average amplitude value, a_n and b_n are amplitudes, and n is the integer multiplier of the fundamental frequency. Harmonics occur as an effect from non-linear loads. Based on signal dispersion in Fourier series (4.1) and notion that the most expressed harmonics on the power grid are the odd number harmonics – the 3rd, 5th and 7th harmonic [34] – the signal distorted by harmonics can be easily obtained. Harmonics should not exceed 5 % of fundamental component amplitude.

The other noise type present in power grids is Gaussian white noise or normal distribution noise. White Gaussian noise is used to simulate all kinds of random processes going on in the system and all systems nearby ranging from radio to cosmic background radiation. The signature feature of this signal is its random nature and standard deviation. The noise signal was chosen with standard deviation of 0.5 and 3 % pu and mean value of 0.

Brownian noise or Brownian motion (also known as *red noise* or *random walk*) is a special kind of noise that is mostly associated with thermal and other

stability issues of devices and measurement systems. Brownian noise can be expressed mathematically as an integral of white noise. Given that ξ_t is a Gaussian random sample value with expected value $\mu = 0$, $X_t = \xi_t$, the Brownian motion is given by:

$$X_t = \int_0^t \frac{\mathrm{d}\xi(\tau)}{\mathrm{d}\tau}\mathrm{d}\tau\,. \tag{4.2}$$

Direct Current (DC) is also a very undesirable component of a modern AC distribution system. DC can be induced in AC network by failure of rectifiers and this adds unwanted current to other devices. DC current can overheat devices and saturate transformers. The final signal is given in Fig. 4.1 with 10 % pu of DC offset.

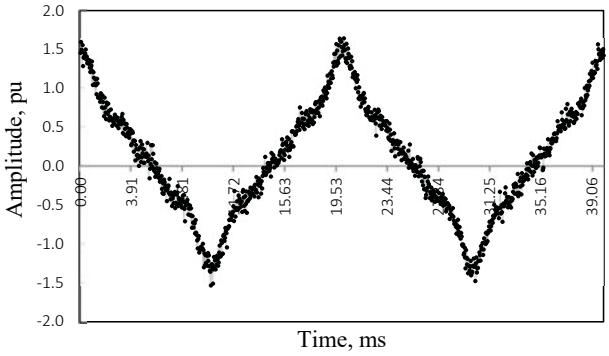

Fig. 4.1. Distorted input signal.

The final generated input signal consists of the following:

- fundamental frequency of 50Hz and amplitude 1 pu;
- harmonics: 3rd, 5th and 7th with amplitude 0.20 pu, 0.12 pu and 0.08 pu, respectively;
- white Gaussian noise with 0.03 pu amplitude and mean value 0;
- DC offset with amplitude 0.1 pu.

4.2 Noise effect on the model

By doing research on noise in distribution systems[1] more realistic values would be:

[1] Experimentally examined in authors MSc. Thesis "Vadāmības traucējumu noteikšana un izpēte zemsprieguma elektrotīklā viedajām mērīšanas sistēmām".

- 0–3 % harmonics;
- 0–1 % noise;
- 0–1 % DC offset.

SEMPR implements no filtering so all the disturbances have effect on the final declared value and estimation process itself. An additive disturbance is implemented. The true nature and mathematical models of the noise processes are still quite unknown. "*Additive noise*" for this model is a property we use to make the model tractable.

At first, a small Gaussian white noise (0.1 %) is added to the 50 Hz signal with an amplitude of 1 pu and ROCOF of 0.3 Hz/s. The sum of the signal and the noise is then fed into SEMPR estimation algorithm. The results are given in Table 1.

Table 1

Estimated values of the input signal with 0.1 % noise

Measurand	Input	Output
Amplitude, pu	1	1.00
Frequency, Hz	50	49.99
ROCOF, Hz/s	0.3	0.33
Phase offset, rad	0	$5.00 \cdot 10^{-5}$

Noticeable error for this measurement is 1 mHz in frequency and 30 mHz/s for ROCOF estimation. This gives GoF value of 69.63 dB.

GoF is a good indication of the quality of the measurement, e.g. 70 dB would indicate that the model used can account at least for 99.999 % of the real world observed. The GoF value decreases once the model cannot account for larger parts of the observed signal, like when phase jumps by 180° or large part of the signal is noise/other disturbances. With GoF it is possible to evaluate each disturbance effect on SEMPR and on the chosen model (Table 2).

Table 2

Estimated values of the input signal with different noises

Measurand model / % pu	GoF, dB (Harmonics)				GoF, dB (Gaussian)				GoF, dB (Brownian)				GoF, dB (DC offset)			
	0.1	*1.0*	*1.5*	*3.0*	*0.1*	*1.0*	*1.5*	*3.0*	*0.1*	*1.0*	*1.5*	*3.0*	*0.1*	*1.0*	*1.5*	*3.0*

Phasor	61	41	37	31	68	49	46	40	37	17	14	8	59	40	36	30
Kirkham equation	61	41	37	31	69	49	46	40	37	18	14	8	59	39	36	30
Kirkham equation with harmonics, DC	304	318	310	307	69	49	45	39	51	29	20	8	264	233	231	246

- The Brownian noise impacts the measurement the most. It is understandable, as random walk increases with time;
- With lesser disturbance to a measurement is the Gaussian noise (the average value should be approaching zero), but since there is no mathematical model to predict noise values (random values), it affects all measurements equally.
- With small ROCOF (comparable to noise signal [26]) values the measurement quality is comparable with phasor model measurements, but one must keep in mind that the small ROCOF values are what we are really after.
- Harmonics and DC offset can be described in the model and therefore improves the measurement for those types of disturbances. For Brownian noise the model assigns at least some of the random walk amplitude to DC offset, so fit for "Kirkham equation with harmonics, DC" slightly improves.

4.3 Allan variance

Allan variance or *two sample variance* is an appropriate way to measure the stability of the estimator in time domain. Allan variance is widely used in precision clock and oscillator industry to measure clock stability due to noise, so the same principles can be applied to SEMPR stability while handling noisy signals.

The Allan variance σ_y^2 , as defined by David Allan and expressed mathematically in [35] and later in [36] as:

$$\sigma_y^2(\tau) = \frac{1}{2\tau^2}\langle(\Delta^2 x)^2\rangle = \frac{1}{2}\langle(\Delta y)^2\rangle, \tag{4.3}$$

where the τ is the measurement interval, and brackets < > denote ensemble average for infinite time. Allan variance is then computed over large strings of measurements

and the more measurements the better is the confidence on the estimate. Usually the calculated Allan variance is plotted as a function of measurement window length and looks as in **Error! Reference source not found.** 4.2 [37]. Increasing of measurement window gives smaller variances but given long enough window lengths a minimum can be achieved after which the variance starts to increase. This is usually caused by drifting parameters or low frequency noise (like Brownian noise).

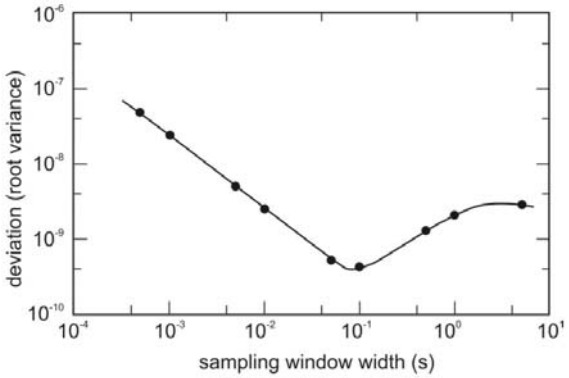

Fig. 4.2. Deviation as a function of measurement length *[37]*.

The notion of constant parameters over the measurement window τ gives opportunity to use Allan variance for SEMPR frequency estimates (constant through whole measurement window). Constant parameters are very doable with synthetic generated signals. This also allows to precisely control the noise parameters and estimate the limitations of the estimator in a sense of resilience to noise and different measurement window lengths τ.

1 % white Gaussian additive amplitude noise on the input signal is considered with different measurement windows.

- Single cycle (0.02 s)
- Double cycle (0.04 s)
- 4 cycle (0.08 s)
- 10 cycles (0.20 s)
- 50 cycles (1.00 s)

The Allan variance can be calculated for all measurement windows. The results for frequency variance are given in Fig. 4.3 where each dot represents **100** measurement variance at 1 % additive white Gaussian noise.

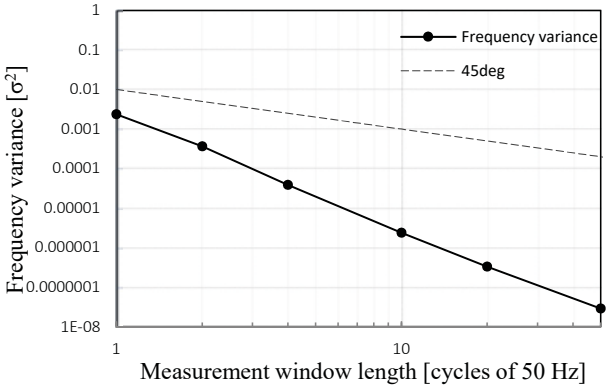

Fig. 4.3. Allan variance for frequency variable as a function of measurement window length.

It can be observed that given larger the measurement window the less the variance and more confidence in the measurement. This comes clearly from the definition of white Gaussian noise characteristics that over larger observation period the mean value approaches 0 and does not affect the variance so much.

By adding larger amplitude noise, the variance would also change. Different white Gaussian noise amplitudes are considered:

- 0.5 %;
- 1.5 %;
- 5 %;
- 15 % ;

and added to the input signal. The results for frequency are given in **Error! Reference source not found.**.

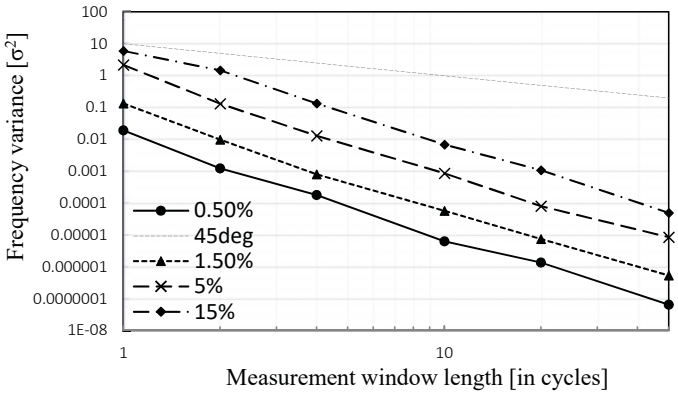

Fig. 4.4. The Allan variance of the frequency values as a function of measurement window length for different noise amplitudes.

Interestingly, independently from noise amplitude frequency estimate keeps the trend and confirms that the frequency estimation would greatly benefit from longer measurement windows.

In power system case a parameter of particular interest is ROCOF. In the generated synthetic data, the ROCOF is set 0 Hz/s, but if the estimator is allowed to search for it, it is possible that there is a value assigned to ROCOF to better fit the model (this should be more pronounced in short-window cases). ROCOF value usually is very small and it gets drowned by noise very fast, so with assigned noise values for Gaussian white noise the estimates for short measurements should be unstable. ROCOF variance as function of measurement window length and with multiple level of noises is given in **Error! Reference source not found.**.

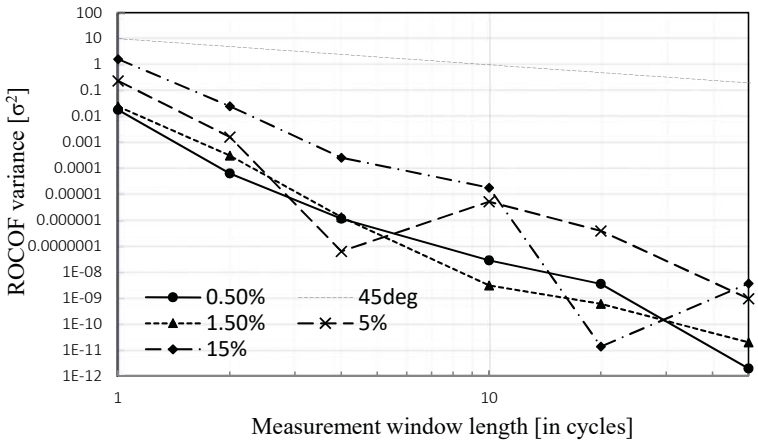

Fig. 4.5. The Allan variance of the rate of change of frequency values as a function of measurement window length for different noise amplitudes.

It is clear that ROCOF benefits from longer observation windows even more than frequency measurement (no surprise here, as ROCOF is frequency derivative). Short measurement windows produce widely variable ROCOF values, even if the ROCOF is constant. This poses the challenge to measure frequency and ROCOF at ever higher speeds and shorter windows. It is possible that ROCOF (about 5 magnitudes smaller than frequency variable [32]) for very short observation windows is not possible to measure in presence of even small noise (comparable to ROCOF itself). The problem is that PMUs are asked to report the values within very short time (couple of cycles).

Just to indicate how the values are varying in Fig. 4.6, frequency values are given for each measurement window length.

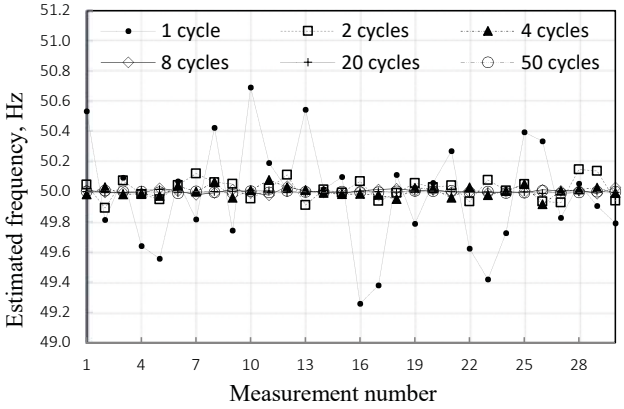

Fig. 4.6. Estimated frequency with 5 % added white Gaussian noise.

Single cycle measurement variance is very large (from 49.2 Hz to 50.2 Hz) and larger measurement windows converge more to 50Hz.

The variance of ROCOF in Fig. 4.7 is given for 50 cycle measurements.

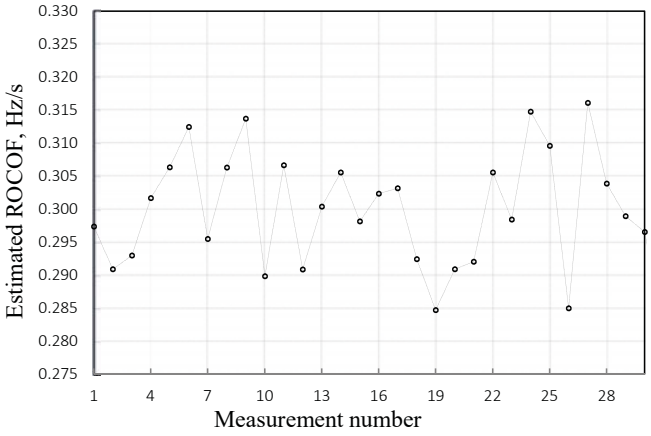

Fig. 4.7. Estimated ROCOF with 5 % added white Gaussian noise and measurement window of 50 cycles.

Considering the difficulty of distinguishing ROCOF from noise, it is very clear, that larger measurement windows reduce this variance and for 50 cycle measurement windows the effect of white noise is reduced and the error is down to 15 mHz/s.

The other type of noise is low frequency Brownian motion or red noise. For Brownian noise, the amplitude levels are selected as:

- 0.009 %;
- 0.03 %;
- 0.5 %;
- 1 %.

For combined additive sample values with Gaussian white noise the results of phase estimation are given in **Error! Reference source not found.** 4.8.

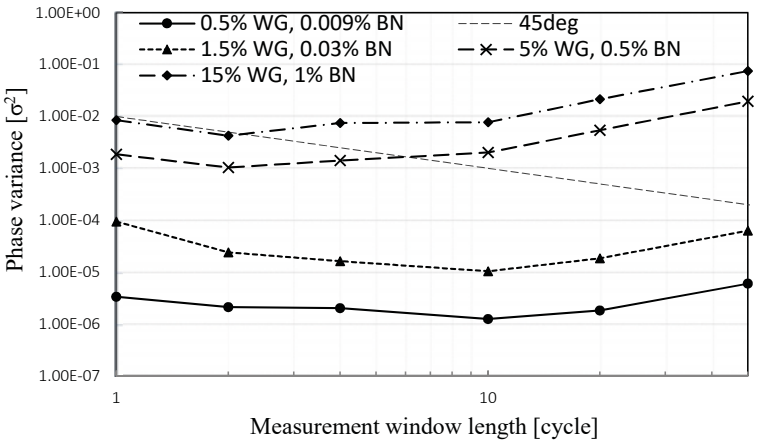

Fig. 4.8. Allan variance of phase measurement affected by different levels of white Gaussian and Brownian noises as a function of window length.

It is evident that a minimum can be observed. With given resolution it appears that the optimum measurement window length for 0.5 % white Gaussian and very small 0.009 % Brownian motion is 10 cycles. For large noise value minimum variance is for 2 cycle-windows. This is mathematical calculation that could be performed in any PMU device as after measurement analysis.

In the next case it was assumed that all noises are additive noise values that were added to signal samples. This gives a lot of variation for signal generation and estimation. By adding different kind of noise to each parameter in Kirkham Equation, it can be observed that the effects are different. With separately added 5 % of white Gaussian noise to amplitude, frequency, ROCOF and phase it can be seen that it affects the Allan variance of each parameter differently.

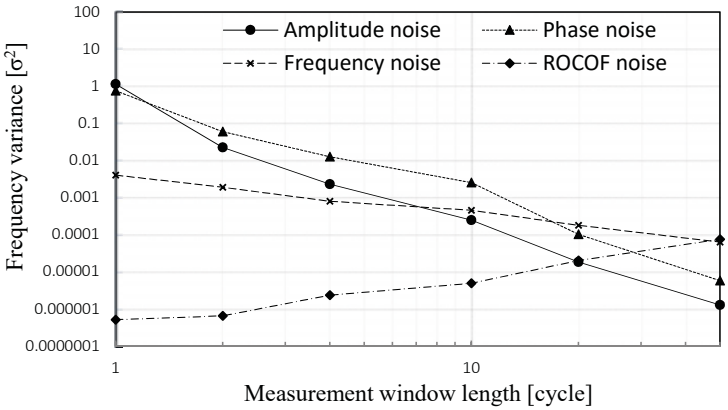

Fig. 4.9. The change of frequency estimation variance by different types of noises for differently sized measurement windows.

- The ROCOF noise results in the smallest variance. This is due to the tiny ROCOF role in the model [26]. However, estimation of ROCOF is very similar to estimation of noise signal, and actually all variances of ROCOF are large.
- The most influential noises are the amplitude noise and phase noise. This is also the reason why they are usually separated and examined as different functions.
- Frequency noise theoretically cannot be distinguished from phase noise, but since it is a derivation of phase noise its influence is reduced below amplitude and phase noises.
- Interestingly, some noises cause an increase in variance in larger observation windows. This is evident with frequency noise for amplitude and phase estimations.
- Even though ROCOF noise influence on the variance is very small, it increases with observation time and by 1 s it has reached the same influence on the estimated parameter variance as other noises. This makes 1 second observation as a boundary where ROCOF and frequency noises could overwhelm amplitude and phase noises. For the lowest variance 1 s could become optimal because, while with increasing measurement windows amplitude and phase noise influence would decrease, frequency and ROCOF would increase, causing the same estimation variance.

4.4 Sampling variance

There are many similar theorems, like Fractional sampling theorem [38], Walsh sampling theorem [39], Zhu sampling theorem [40] and others, just to mention

few. The fact that there are so many related theories and topics points out the significance of signal processing to the modern technology for communication, control, and processing applications. However, all theories trace back to Harry Nyquist [41] and Claude Shannon [12].

If the signal $f(t)$ is band limited, then it can be fully described by denumerably infinite set of values equally spaced by $1/2W$ seconds (if a function $f(t)$ contains no frequencies higher than W cps)

$$f(t) = \sum_{n=-\infty}^{\infty} \left(\frac{n}{2W}\right) \frac{\sin 2\pi W \left[t - \left(\frac{n}{2W}\right)\right]}{2\pi W \left[t - \left(\frac{n}{2W}\right)\right]}, \tag{4.4}$$

where n is the sample value obtained by sampling. Spectrum of such signal $f(t)$ outside band W is zero.

The main problem with real-world applications is that no real signal is perfectly band limited nor filtered to be perfectly band limited. In fact, in order for a signal not to have any energy outside finite frequency band, it must be infinite in time.

This is something that designers of PMU systems have kept in mind knowingly or unknowingly, because each and every manufacturer chooses his own approach. In real devices the sampling rate can be from 24 samples to 512 samples per cycle. This begs the question – are we doing oversampling in PMUs? Sampling rate nowadays is something that can be changed by a software (firmware) change so it is very doable, so what would be the optimum sampling rate? In theory it can be deducible with measurements and their variance.

In 1968, Karl Johan Åström in [42] discussed different sampling rates or time analysis of N samples at equal spacing h. By considering a stochastic differential equation

$$\mathrm{d}x = -\alpha x \mathrm{d}t + \mathrm{d}w, \tag{4.5}$$

where α is a parameter to be estimated, $\{w(t)\}$ is random walk (Wiener process), and values x are observed at sampling intervals with equal spacing h. The smallest variance is then mathematically calculated and shown in Fig. 4.10.

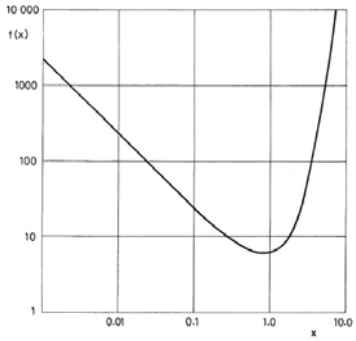

Fig. 4.10. Graph of the function $f(x) = (e^{2x} - 1)x^{-2}$. The variance of the estimate α using N values with the spacing h is $\alpha^2 f(\alpha h)/N$ [42]..

The optimum sampling choice is h_0 – 0.797/α, which gives the smallest variance of $\hat{\alpha}$. The variance of $\hat{\alpha}$ increases significantly for sampling rates lower than h_0 (larger sampling intervals).

Considering the practical implementation of SEMPR, it should be also possible to determine the optimum sampling frequency based on the components (harmonics and noise, not only Wiener process) in the signal. In such case the optimum for the sampling rate would also be very well described by a variance value, but instead of changing observation time, one would change the sampling rate. It should be possible to determine the optimum experimentally by implementing SEMPR. Sampling variance then can be expressed similarly to Allan variance, but instead averaging the measurements over increasing time period, we can average measurement over the increasing sample number, but keep measurement window the same.

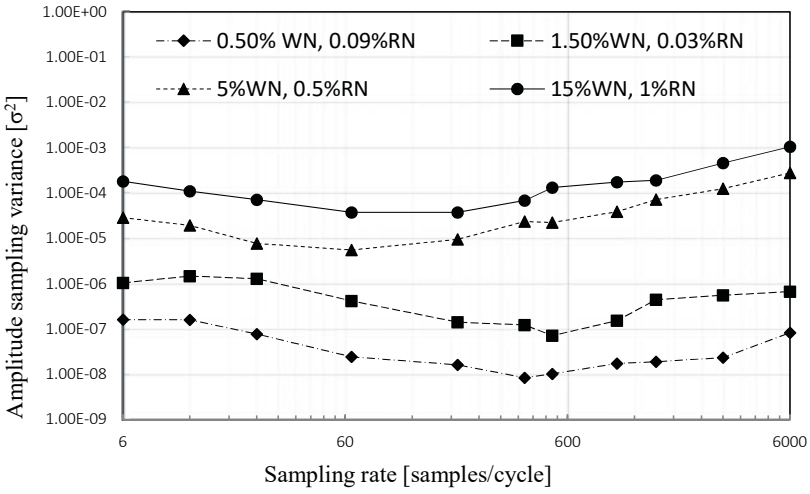

Fig. 4.11. Sampling rate variance for Amplitude estimation.

Simulation results show an interesting trend that includes a minimum condition for variance. The following observations can be made.

- The optimal sampling frequency decreases with larger noise influence. This can be partially explained by the effect of the noise over fewer or larger sets of sampling values. Fewer samples can ignore more noise, therefore improve the fit numbers and decrease the variance.
- With fairly plausible noise levels (0–3 %) the optimum sampling frequency is in fact somewhere between 192 and 512 samples per cycle (in this simulation closest point is 384 samples per cycle). This is in the same category as for micro-PMU, therefore their sampling frequency could be around optimum.

This also shows that under-sampling and over-sampling should be avoided and by purely mathematic calculations it is possible to find an optimum sampling frequency based on the typical signal that the device should be observing.

Chapter 5. Experimental Data Analysis

During the research in the United States of America the real-world point on wave data was shared by AEP (American Electric Power) power network. Unfortunately, all attempts to get similar data from Latvian transmission system operator AST (JSC "Augstsprieguma tīkls") were unsuccessful as they were met by silence. Therefore, with the permission from Alex McEachern from Power Standards Laboratory, all anonymized real data analysis was done with available EHV (345 kV 60 Hz) system data.

Processes during fault are of a particular interest and the reconstructed waveform can be observed in Fig. 5.1. Notice that the amplitude for the second cycle of measurement window in phase C is significantly low, and SEMPR should be able to accommodate for that with ROCOA (rate of change of amplitude). During the fault in phase C the fault current exceeds 500 A.

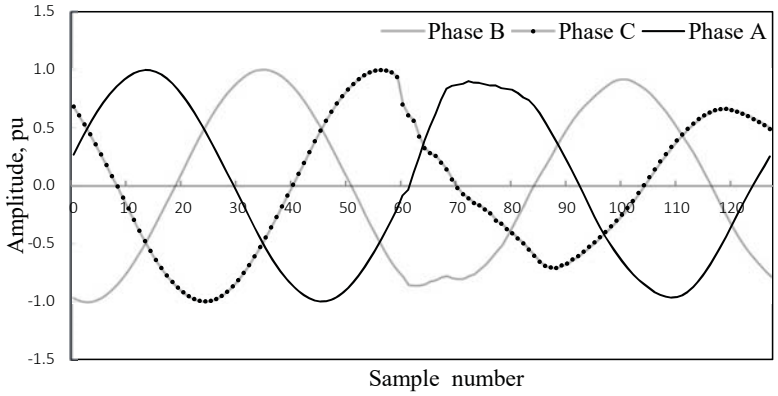

Fig. 5.1. Fault in 345kV EHV three phase system.

Reported phasor values of the industrial PMUs also are provided so GoF can be calculated and PMU performance can be determined. For steady state couple of cycles before the fault the GoF level of the measurement is 34.88 dB. Residual peak values are around 0.03 pu or 3 % of the fundamental.

Estimation, signal reconstruction and GoF calculation is performed to 1 second worth of data and are depicted in Fig. 5.2. Plotted along GoF values are the current values to indicate fault duration.

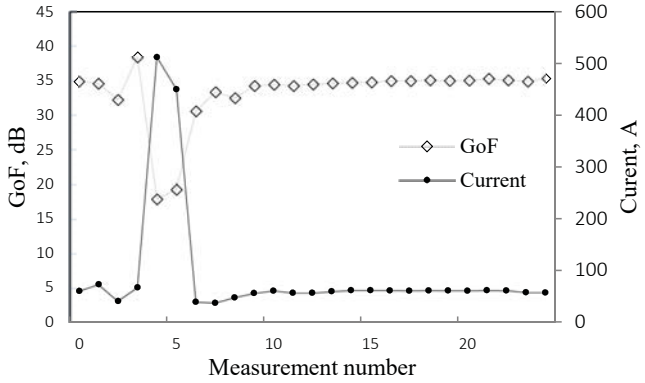

Fig. 5.2. Goodness of Fit for 60 measurements with corresponding current measurements for phase C.

During fault the GoF values decrease significantly (approximately 20 dB) and current increase corresponds well with obtained measurements. Note that the GoF values during normal operation are more or less consistent and residual values are as well. This indicates a constant slight mismatch in phase for which at this point the source is unclear (presumably timing in the device).

5.1 Real data estimation vs the models

The main advantage of SEMPR is that the model is selectable freely, so different models can be applied (also with capabilities to run them simultaneously as parallel processes). At least 3 models are worth looking at:

- phasor model (2.2);
- Kirkham model without ROCOA;
- Kirkham model with ROCOA (3.1).

All measurements are performed with the same 2-cycle measurement windows and the same 1 second real-world input data (phase C). GoF metric for measurements is given in Fig. 5.3.

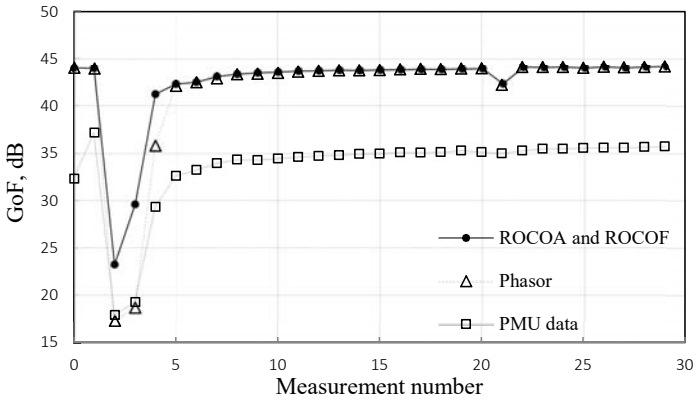

Fig. 5.3. GoF calculation for SEMPR measurements compared to PMU declared value GoF calculation.

In this example SEMPR can achieve better signal representation, especially during fault conditions. Over nominal operation SEMPR produces results on average 8 dB better than PMU values, but over fault there is 11 dB difference. Close Gof values over steady state indicates that over nominal conditions a phasor is also a very good representation of the real world.

Estimated values during fault (measurement No. 3) is 1.072 pu for amplitude, –28.848 pu/s for ROCOA, 60.639 Hz for frequency, –33.727 Hz/s for ROCOF, and 46.071° for phase. This means that for amplitude SEMPR estimates that the voltage is dropping by astonishing 28 pu per second, or 0.23 pu per cycle. This means that in one cycle voltage level is estimated to decrease by at least 81 kV. ROCOF value also indicates slowing down of the sine-wave by 33 Hz per second.

When plotted together the signal is given in Fig. 5.4.

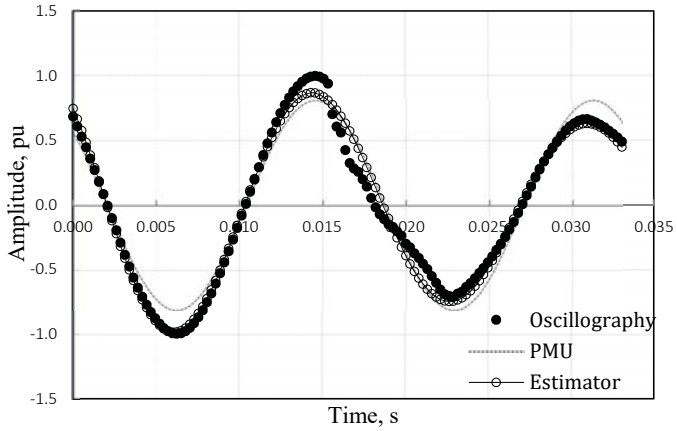

Fig. 5.4. SEMPR algorithm reconstruction along with PMU reconstruction and real oscillography data.

It is evident that SEMPR makes better estimation of the signal, and for large parts of input data the estimation and oscillography lines are indistinguishable while PMU data reconstruction underestimates the peak values in the first half of the measurements and overshoots in the second.

5.2 Real data variance analysis

The same AEP data used were considered for fault measurement analysis. The fault occurs at the beginning of almost one second worth of sample set. A PMU looks at the fault in two cycle measurement windows, but SEMPR can look at it even at half-cycle windows and 4 cycle windows (using model of a phasor). With measurement window decreasing we seemingly get more detail, but with half-cycle reported values we also get very high variance over the data where the fault occurred and the frequency at first jumps to 68 Hz and then plummets to 52 Hz giving 16 Hz difference between two adjacent half-cycles, which just not make sense (not physically possible). The signal only vaguely resembles sine-wave, so measurements only vaguely resemble sensible information.

It is important at this stage to look at the SEMPR and the meaning of the measurement. First, 52 Hz is what apparently gives the least amount of residuals. Second, we are looking for coefficient in a phasor model (2.2) and by the looks of it, the signal is not a phasor. Our model for representing the nature makes no sense. We get that indication also from GoF that for the measurement producing 52 Hz is 26 dB, instead of steady 44 dB for the rest of data set.

For further analysis, unfortunately, AEP data is not suitable to sensibly represent Allan variance calculations, there simply is not enough data. Larger data chunks were made available by a μPMU device [21] sampling at 512 samples per cycle and providing 30 seconds worth of data in medium voltage distribution grid. By the analysis of the data it is very noisy and after spectral analysis the signal contains 3rd, 5th and 11th harmonic as well as high frequency noise. Since the data set is from normal system operation period, the values should be quite stationary and Allan variance can be calculated (Fig. 5.5).

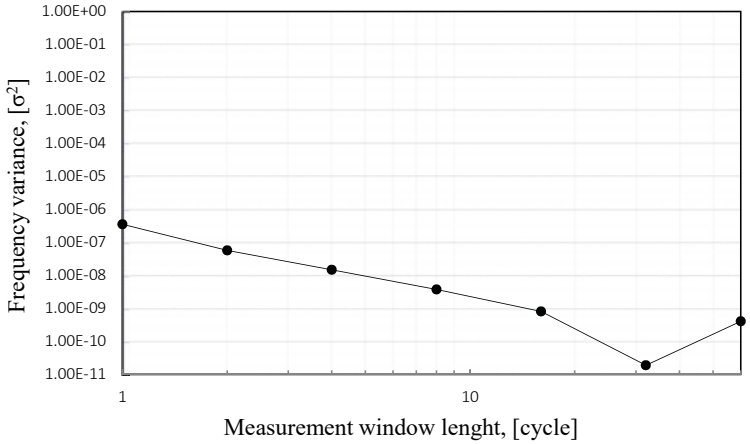

Fig. 5.5. Allan variance for distribution network frequency measurements.

Each dot represents an Allan variance calculated from different number of measurements since the data set is finite. There is a distinctive minimum at 32 cycle measurement window, which would give approximately half a second frequency reporting time, well below what is expected from PMU.

Chapter 6. Conclusions

The notion that the process of measurement is in fact the same as solving an equation lends itself well for examination with time-varying signals. The "experiment" of making a measurement by curve-fitting proves that the act of measuring is one that can be done in various ways, but the end result should not depend on the method selected. Most importantly, it teaches that measurement is the act of using signals from the real world to find parameters of a model. That model is almost always a simplification.

The idea of measurement being the same as solving an equation gives more room for improving and adjusting our conceptual models for reality observed. In this

case a Kirkham equation is used instead of just a phasor to show its advantages in real-world applications. This gives PMUs added degrees of freedom for amplitude and frequency to account for time-varying signal that is in power system.

PMUs now are one of the most influential modern measurement devices especially for stability-challenged power systems. For the same system control and supervision targets it could be possible to also use PMUs in distribution network. Of course, strong communication backbone is essential for synchronized measurements.

Research shows that PMUs struggle with signals under transition process. This caused the amending of the PMU standard at IEEE. This should not be so, and PMUs must report something. It is suggested to use GoF to validate the trust regions for such reports.

SEMPR produces independent measurements utilizing no filtering. For proof of concept synthetic data is analyzed and shows flawless results.

A metric called Goodness of Fit is introduced and integrated in SEMPR. The Goodness of Fit parameter, developed from an idea in [5], has showed potential to be very useful with real PMUs and real signals. It indicates in real time the degree of match between the signal (changing with the power system), and the measurand (fixed by the design of the PMU). GoF level can be calculated by any PMU and the calculation is straightforward, it does not depend on the measurement method. The GoF indicates that near-ideal results can be obtained with an ideal signal. GoF is proved to be a promising technique for a large class of digital measurements.

When tested with different noises, it shows that Brownian noise has the greatest impact on measurement. There is less impact for white Gaussian, but for harmonics we can adjust the model and the impact is minimized.

From performed calculations it has been showed that ROCOF is actually a tiny variable in the mathematical model and its contribution to the final signal is down to noise levels. More research in noise and its effects on the model could be performed to further improve the ROCOF measurement. It seems quite meaningless before we improve our understanding [43].

By implementing the Allan variance method the frequency and ROCOF measurements show great benefit from longer measurement windows (significantly more than amplitude or phase).

With introducing synthetic semantic coloration (Brownian noise) and based on Allan variance calculations, an optimum emerges for optimum window lengths. The optimum changes according to the contents of the signal (noise content and amplitude), e.g. for phase measurement with smaller noise amplitudes (up to 1.5 % white Gaussian (WG) and 0.3 % Brownian (B)) the optimum is around 10 cycles, but for larger amplitudes (up to 15 % WG and 1 % B) around 2 cycles. For more typical

1.5 % WG and 0.03 % B noise levels an optimum was found for 512 samples per cycle which is what μPMU uses in [21].

An additional statistical analysis tool has been proposed, called “sampling variance”. It is showed that an optimum also exists for sampling rate, depending on the signal and noise content. For smaller noise amplitudes (0.5 % WG and 0.09 % B) the optimum sampling frequency is 384 samples per cycle, but for large noises (15 % WG and 1 % B) optimum is quite flat – around 100 samples per cycle.

Based on real-world data and SEMPR results, it has been proven that PMU devices are actually solving a phasor equation. A lot of time power system signals do not resemble a phasor. GoF metric shows that Kirkham equation would be a better option, since more degrees of freedom are provided for signal to change. Using Kirkham model showed a 6 dB increase in GoF (14 % increase since steady state GoF is around 43 dB) over the fault data.

When variance techniques are applied to obtained real world data, it shows that shorter observation windows are not necessarily better than sensible compromise. Considering small impact of ROCOF signal on the total result and high disturbance content on signal during fault, it is actually useless to use mathematical model of a phasor in real-world measurements. As short as half-cycle measurement windows are used with the largest variance.

Future Research on the Topic

Statistical analysis is something that PMU also can do just like GoF calculation. In this case it is possible to adjust the conceptual model (including observer notification, of course), window length (possible multiple measurement windows at the same time), sampling frequency to achieve best possible representation of the real signal (maximum GoF value). Such device would perform informed and intelligent measurements providing more information about the nature to the observer.

One of the findings is that the noise in the power system is not a very researched topic and true nature of the disturbances is still quite unknown. As the matter of fact, also the power system signals under fault conditions are yet to be studied and not only curve fitting but pattern recognition approach may be suggested. This way it would be possible to get ever better GoF values and increase our understanding about the true nature of the physical phenomena in real time.

Real PMU with GoF integration is under way [9], therefore more data and possible findings are possible. With reported GoF values along with declared parameter values will bring knowledge to the observer whether to trust or discard the measurement, and in power system operations this is huge improvement.

Bibliography

[1] Engineering and Technology History Wiki, «2007 IEEE Conference on the History of Electric Power,» 2007. [Online]. Available: https://ethw.org/2007_IEEE_Conference_on_the_History_of_Electric_Power.

[2] Ramsey, W. «The Largest Machine Ever Built and It's Under Press," Warren Rural Electric Corp, 2014. [Online. Available: http://d2i9dixktx83yv.cloudfront.net/wp-content/uploads/2014/02/CEO-column-January-2014-updated-1-13-131.pdf. [2018].

[3] Tiatiushkin, A. "kep power testing blog," 2016. [Online]. Available: http://kep-power-testing-blog.blogspot.com/2016/10/the-worlds-electrical-power-grid-as.html. [2018].

[4] Phadke, A. G., Thorp, J. S., Adamiak, M. G. "A new Measurement Technique for Tracking Voltage Phasors, Local System Frequency, and Rate of Change of Frequeuncy," *IEEE Transactions on Power Apparatus and Systems,* no. 5, p. 1025-1038, 1983.

[5] NASPI, "North American SynchroPhasor Initiative," 2018. [Online]. Available: https://www.naspi.org/.

[6] Von Meier, A., Culler, D., d McEachern, A. "Micro-synchrophasors for distribution systems" *Innovative Smart Grid Technologies Conference*, Washington, DC, USA, 2014.

[7] "IEEE Std. C37.118.1-2011 Standard for Synchrophasor Measurements for Power Systems," *IEEE Standard,* 2011.

[8] IEEE Power and Energy Society, "IEEE Std C37.118.1a-2014 Modifictaion of Selected Performance Requirements," 2014.

[9] Laverty, D. M., Kirkham, H., Morrow, D. J., Liu, X. "Estimation of goodness of fit of synchrophasors during transient faults," *2017 IEEE Power & Energy Society General Meeting*, Chicago, USA, 2017.

[10] Rutman, J. "Characterization of phase and frequency instabilities in precision frequency sources: Fifteen years of progress," *Proceedings of the IEEE,* vol.66, no. 9, 1978.

[11] Rutman, J., "Oscillator Specifications: a Review of Classical and New Ideas," *31st Annual Symposium on Frequency Control*, Atlantic City, USA, 1977.

[12] Shannon, C. "A mathematical theory of communication," *The Bell System Technical Journal,* Vol.27, no. 4, p. 623-656, 1948.

[13] Kirkham, H., Riepnieks, A. "Measurement of Phasor-like Signals," Pacific Northwest National Laboratory, Richland, USA, 2016.

[14] Phadke, A. "Synchronized phasor measurements in power systems," *IEEE Computer*

Applications in Power, Vol. 6, no. 2, p. 10-15, 1993.

[15] Sauhats, A., Svalova, I., Svalovs, A., Antonovs, D., Utans, A., Bochkarjova, G. "Two-terminal out-of-step protection for multi-machine grids using synchronised measurements," *2015 IEEE Eindhoven PowerTech*, Eindhoven, Netherlands, 2015.

[16] Antonovs, D., Sauhats, A., Utans, A., Svalovs, A., Bochkarjova, G. "Protection scheme against out-of-step condition based on synchronized measurements," *2014 Power Systems Computation Conference*, Wroclaw, Poland , 2014.

[17] Yong Li, Dechang Yang, Fang Liu, Yijia Cao, Christian Rehtanz, Interconnected Power Systems: Wide-Area Dynamic Monitoring and Control Applications, Springer, 2015.

[18] Raymond H.Byrne, Ricky J. Concepcion, Jason Neely, "Small signal stability of the western North American power grid with high penetrations of renewable generation," *Photovoltaic Specialists Conference (PVSC)*, Portland, 2016.

[19] Project Group Turkey, "Report on Blackout in Turkey on 31st March 2015," European Network of Transmission System Operators for Electricity, Brussels, 2015.

[20] R. d. Vries, *Phasor Measurement Units (PMUs) and time Synchronization at European Utilities.* [Performance]. Arbiter, 2013.

[21] Von Meier, A., Culler, D., McEachern, A. "Micro-synchrophasors for distribution systems," *Innovative Smart Grid Technologies Conference (ISGT)*, Washington DC, 2014.

[22] Gheen,K. *Phase Noise Measurement Methods and Techniques.* [Performance]. Agilent Technologies, 2012.

[23] Dickerson, W. "Effect of PMU analog input section performance on frequency and ROCOF estimation error," *IEEE International Workshop on Applied Measurements for Power Systems*, Aachen, Germany, 2015.

[24] Goldstein, A. *Lessons learned from the NIST assessment of PMUs.* [Performance]. National Institute of Standards and Technology, 2014.

[25] Gerard Stenbakken, Ming Zhou, "Dynamic Phasor Measurement Unit Test System," *Power Engineering Society General Meeting*, Tampa, USA, 2007.

[26] Riepnieks, A., Kirkham, H. "Rate of change of frequency masurement," *Power and Electrical Engineering of Riga Tecnical University (RTUCON)*, Riga, 2016.

[27] Jacques Rutman, Walls, F. L. "Characterization of Frequency Stability in Precision Frequency Sources," *Proceedings of the IEEE,* Vol. 79, nr. 6, 1991.

[28] Boashash, B. "Estimating and interpreting the instantenious frequency of a signal. I. Fundamentals," *Proceedings of the IEEE,* vol.80, no. 4, 1992.

[29] Kirkham, H. "A conceptual Framework for Measurement (with emphasis on phasor measurement)," Pacific Northwest National Laboratory, Richland, USA, 2015.

[30] Kirkham, H., Riepnieks, A., McBride, E. So. J. "Error correction: A proposal for a standard," *2016 Conference on Precision Electromagnetic Measurements*, Otawa, Canada, 2016.

[31] T. M. Inc., ""Documentation"," 2018. [Online]. Available: http://www.mathworks.com/help/matlab/.

[32] Riepnieks, A., Kirkham, H. "An Introduction to Goodness of Fit for PMU Parameter Estimation," *IEEE Transactions on Power Delivery,* Vol. 32, no. 5, p. 2238-2245, 2017.

[33] Cuthbert, D., Wood, F. S. "Fitting Equations to Data", New York, USA: Wiley, 1971.

[34] Shah, N. "Whitepaper: Harmonics in power system. Causes, effects and control," May 2013. [Online]. Available: https://www.industry.usa.siemens.com. [Accessed 2018].

[35] Allan, D. W. "Statistics of atomic frequency standards," *Proceedings of the IEEE,* Vol. 54, no. 2, p. 221-230, 1966.

[36] Allan, D. W., Ashby, N., Hodge, C. "The Science of Timekeeping," Hewlett-Packard Company, 1997.

[37] Kirkham, H., Riepnieks, A. "Dealing with non-stationary signals: Definitions, considerations and practical implications," *Power and Energy Society General Meeting*, Boston, USA, 2016.

[38] Torres, R., Lizarazo, Z., Torres, E. "Fractional Sampling Theorem for -Bandlimited Random Signals and Its Relation to the von Neumann Ergodic Theorem," *IEEE Transactions on Signal Processing,* Vol.62, no. 14, pp. 3695-3705, 2014.

[39] Splettstober, W. "Error Analysis in the Walsh Sampling Theorem," *1980 IEEE International Symposium on Electromagnetic Compatibility*, Baltimore, 1980.

[40] Zhai, J., Zhang, L., Yu, Z. "Digital predistortion of RF power amplifiers with Zhu's general sampling theorem," *2015 Asia-Pacific Microwave Conference*, Nanjing, 2015.

[41] Nyquist, H. "Certain Topics in Telegraph Transmission Theory," *Transactions of the American Institute of Electrical Engineers,* Vol.47, no. 2, p. 617-644, 1928.

[42] Åström, K. J. "On the Choice of sampling rates in Parametric Identification of Time Series," Lund Institute of Technology division of automatic control, Lund, Sweden, 1968.

[43] Kirkham, H., Pandey, S. "Is ROCOF measureable?", *2018 IEEE Power & Energy Society Innovative Smart Grid Technologies Conference (ISGT)*, Washington, USA, 2018.

Artis Riepnieks was born in 1988. He obtained the Bachelor degree in Telecommunications, Power and Electrical Engineering and Master degree in Computerized Control of Electrical Technology from Riga Technical University, Latvia. From 2011 to 2015, he held a position of smart grid technology engineer at JSC "Latvenergo" and JSC "Sadales tīkls" and from 2015 to 2016, he was carrying out research on phasor measurements at Pacific Northwest National Laboratory, USA.
Currently Artis Riepnieks is Head of Customer Service Systems Unit of JSC "Sadales tīkls".